PHYSICAL REVIEW E **93**, 011301(R) (2016)

From measurements to inferences of physical quantities in numerical simulations

Tota Nakamura
College of Engineering, Shibaura Institute of Technology, Saitama 337-8570, Japan
(Received 5 June 2015; revised manuscript received 16 December 2015; published 8 January 2016)

We propose a change of style for numerical estimations of physical quantities from measurements to inferences. We estimate the most probable quantities for all the parameter region simultaneously by using the raw data cooperatively. Estimations with higher precisions are made possible. We can obtain a physical quantity as a continuous function, which is processed to obtain another quantity. We applied the method to the Heisenberg spin-glass model in three dimensions. A dynamic correlation-length scaling analysis suggests that the spin-glass and the chiral-glass transitions occur at the same temperature with a common exponent ν. The value is consistent with the experimental results. We explained a spin-chirality separation problem by a size-crossover effect.

DOI: 10.1103/PhysRevE.93.011301

Introduction. Estimations of physical quantities in numerical simulations are based on equilibrium statistical physics [1]. We virtualize a model system in a computer and perform independent measurements on the system using a definition of a physical quantity. When an evaluation process is complex, both systematic and statistical errors are accumulated in the obtained data. We sometimes encounter numerical instabilities. Then, further analyses become difficult. In what follows, we explain the situation using a correlation-length estimation.

An estimation formula for a correlation length, ξ, is given by the second-moment method: $\xi = \sqrt{\chi_0/\chi_k - 1}/k$ [2]. Here, χ_0 denotes the susceptibility and χ_k its Fourier transform with k as the lowest wave number of the system. This expression itself is problematic. Both the numerator and the denominator of this expression approach zero as the system size increases ($k \to 0$), where this formula becomes exact. We encounter the numerical instability caused by the expression 0/0. In order to avoid this problem, Belletti *et al.* [3] proposed the reduction of this instability by estimating ξ by I_2/I_1 with the integrals $I_k = \int_0 dr\, r^k f(r)$ [r denotes distance and $f(r)$ the correlation functions]. Suwa and Todo [4] proposed a generalized moment method for gap ($\Delta \sim 1/\xi$) estimation in quantum systems. Systematic errors and ambiguity caused by small-size data are eliminated.

Recently, big-data handling has become possible due to a rapid increase in computational power. One estimates unknown quantities, checks modeling assumptions, and makes a prediction for future events out of observed data. This procedure is called an inference in statistics. Probabilistic numerics [5] have been developed in order to improve performance of the inference. Since we follow the same procedure in numerical studies of statistical physics, applications of probabilistic numerics are considered promising. Therefore, the topic of Bayesian inference has been attracting considerable interest [6,7]. In this context, Harada [8] introduced Bayesian inference into a *parameter estimation* of the finite-size scaling analysis.

In this Rapid Communication, we extend its application to *estimations of physical quantities*. The correlation length is estimated directly from the correlation-function data with a much-improved accuracy. We can obtain a continuous function for an energy out of the discrete raw data. It is analytically differentiated to obtain the specific-heat function. Since raw data are cooperatively utilized in this inference procedure, we can reduce numerical errors and avoid numerical instabilities.

We also explain in this Rapid Communication contradictory arguments on a spin-glass transition by a size-crossover effect. Hukushima and Campbell [9] reported in the Ising spin-glass model that there exists a crossover size, $L \sim 24$, where the finite-size effect of the correlation-length ratio, ξ/L, changes its trend from increasing to decreasing. In the $\pm J$ Heisenberg spin-glass model [10], the chiral-glass susceptibility of sizes smaller than $L = 39$ increases with the system size but that of larger sizes decreases. A similar size-crossover effect was also observed in a random quantum spin chain [11,12]. Short-range spin correlations suggest that the energy gap is finite, whereas the long-range ones exhibit behaviors that the energy gap is zero. The size-crossover effect may influence a final physical conclusion.

Method. Let us first explain a method in a tutorial model. We performed equilibrium simulations in a two-dimensional Ising ferromagnetic model, and obtained an energy, E_i, and a magnetization, M_i, at each temperature, T_i, where i is the data index. The linear system size is 999, and it is set to 1999 in the vicinity of a transition temperature. These data are depicted in Fig. 1 by circle symbols. Now, our purpose is to obtain $E(T)$ and $M(T)$ as continuous functions. We apply the Gaussian kernel regression [8,13] using three variables, x_i, y_i, and ϵ_i, defined as

$$x_i = \ln|T_i - T_c|,$$
$$y_i = \ln(-E_i) \qquad (y_i = \ln|M_i| \text{ for } M),$$
$$\epsilon_i = (\delta E_i/E_i)^2 \qquad [\epsilon_i = (\delta M_i/M_i)^2 \text{ for } M].$$

Here, δE_i and δM_i denote errors for E_i and M_i, and T_c denotes a critical temperature that is to be estimated in the following analysis. We defined a Gaussian kernel function as $K(x_i,x_j) = \theta_0^2 \exp[-\frac{(x_i-x_j)^2}{2\theta_1^2}] + \theta_2^2$, where θ_0, θ_1, and θ_2 are hyperparameters. A generalized covariance matrix is $\Sigma_{ij} = \epsilon_i\delta_{ij} + K(x_i,x_j)$. Then, the following log-likelihood function is to be maximized: $\ln\mathcal{L} = -\frac{1}{2}\ln|2\pi\Sigma| - \frac{1}{2}y_i\Sigma^{-1}_{ij}y_j$. This function is defined independently for both $T_i > T_c$ and $T_i < T_c$, and we take a summation of them. The hyperparameters, $\{\theta_0,\theta_1,\theta_2\}$, are also defined independently for two regions. We obtained seven parameters, one T_c and two sets of $\{\theta_0,\theta_1,\theta_2\}$, that maximize $\ln\mathcal{L}$ by the downhill simplex method [14]. We tried this search for 400 times by changing the initial values of the parameters. We estimated averages and error bars for

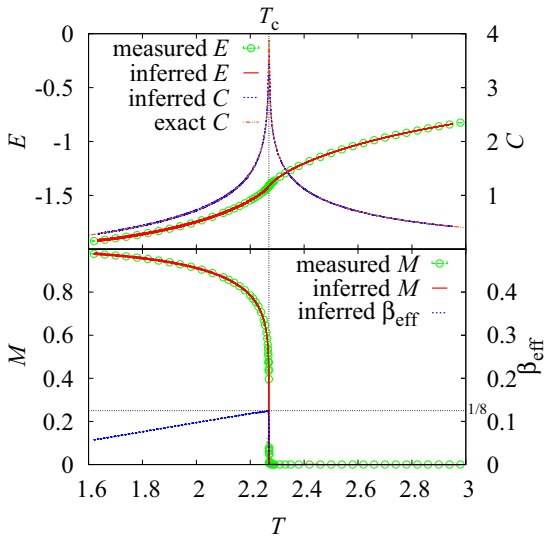

FIG. 1. Temperature dependencies of energy(E), magnetization (M), the specific heat (C), and the effective critical exponent $\beta_{\rm eff}$ in the two-dimensional Ising ferromagnetic model. Error bars are smaller than the symbols and line widths.

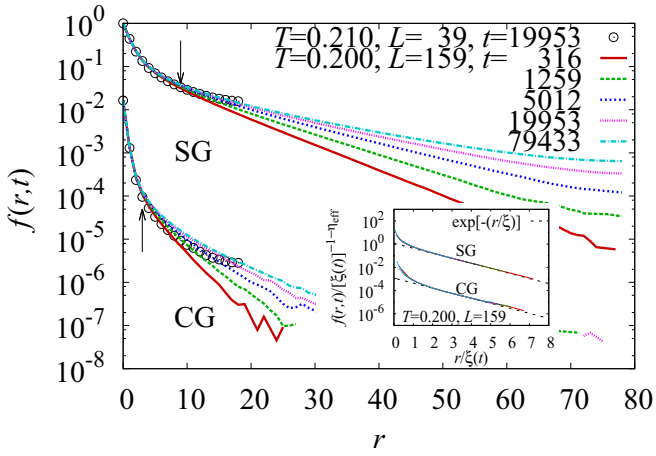

FIG. 2. Correlation function data for selected time steps for $L = 39$ (circles) and $L = 159$ (lines). Arrows depict crossover distances between short-range correlations and long-range correlations ($r_c = 9$ for SG and $r_c = 3$ for CG). Inset: Scaled correlation functions for data with $T = 0.200, L = 159$ depicted with the same line color.

parameters over them. The critical temperature is obtained as a parameter that separates the data into two regions, where the data are fitted most smoothly. It was $T_c = 2.269\,14(4)$ for the E inference and $T_c = 2.269\,19(4)$ for the M inference. They agree with the exact value: $T_c = 2.269\,185\,3\ldots$. Using the obtained parameter set, we write an inference function for E as

$$E(T) = -\exp\left[K(x,x_i)\Sigma_{ij}^{-1}y_j\right], \qquad x = \ln|T - T_c|, \quad (1)$$

where the summations over i and j are taken. We can differentiate this function *analytically*, and we obtain the specific heat, $C(T) = \frac{dE}{dx}\frac{dx}{dT}$, as a continuous function. The inference results for $E(T)$ and $C(T)$ are depicted by lines in Fig. 1. We confirmed that the $C(T)$ function is consistent with the exact results. We obtained a function for M in the same manner. Since $M \sim (T_c - T)^{\beta}$, the effective β is given by $\beta_{\rm eff} = \frac{dy}{dx}$ with $y = \ln|M(T)|$. A critical exponent $\beta = 1/8$ is a value at $T = T_c$. A critical region, where $\beta_{\rm eff}$ approximately equals to $1/8$, was very narrow in this figure.

The nonequilibrium relaxation method [15–18] was proposed to treat large systems in a simple and easy manner. This approach has been applied successfully in random systems [10–12,18–21]. The dynamic correlation-length scaling method [22] was proposed as a variation of this method. We use this method together with the inference method to clarify the spin-chirality problem in the Heisenberg spin-glass model in three dimensions.

Model. A spin glass is a disordered magnet characterized by frustration and randomness [23,24]. One of the most important and unsolved problems in spin-glass studies is the coupling or separation of the spin-glass (SG) degrees of freedom and chiral-glass (CG) degrees of freedom [19,25–42]. Kawamura [26,27] introduced the chirality scenario, wherein the CG order exists without the SG order. There is another scenario, in which the SG and CG transitions occur simultaneously. In 2009, two studies [39–41] on this topic drew two opposite conclusions even though the authors in each case performed similar amounts of simulations, but treated the finite-size effects differently. The present situation suggests that we need considerably larger system sizes to address this problem.

Our model Hamiltonian is $\mathcal{H} = -\sum_{\langle i,j\rangle} J_{ij}S_iS_j$. The summation runs over all the nearest-neighbor spin pairs. The interactions J_{ij} take on two values, $\pm J$, with the same probability. The temperature T is scaled by J. The model is defined on a simple cubic lattice of the form $N = L \times L \times (L+1)$ with $L = 159$. The skewed periodic boundary conditions were applied. We calculated the SG and CG susceptibility, $\chi_{\rm SG}$ and $\chi_{\rm CG}$; SG and CG correlation functions, $f_{\rm SG}$ and $f_{\rm CG}$; and SG and CG correlation length, $\xi_{\rm SG}$ and $\xi_{\rm CG}$. One Monte Carlo (MC) step consists of one heat-bath update, 1/20 Metropolis updates (once every 20 steps), and 124 over-relaxation updates. All the random bond configurations are different at each temperature. A typical sample number at one temperature is 20. More samples are treated near and above the transition temperature. In the study, we ran simulations at 42 sets of temperatures, and the total sample numbers were 1168. We evaluated the order parameters using 435 overlaps among 30 real replicas. At some lower temperatures, we evaluated them using 1128 overlaps among 48 real replicas and checked for consistency regarding the replica number. In the nonequilibrium relaxation study on the spin glasses, the thermal average is replaced by the replica average [22]. The replica number needs to be larger than the value in the equilibrium simulations. Numerical error bars were estimated in regard to the sample average.

Results. We prepared the relaxation data of correlation functions, $f(r,t)$ [t denotes the measuring time step], obtained in the conventional measurement scheme. Figure 2 shows the SG and CG correlation functions for typical time steps in the range from $t = 316$ to 79 433. The temperature, $T = 0.200$, is close to the transition temperature. We also plot the small-L ($L = 39$) data at $T = 0.210$ as shown by circles. The inverse of the slope of the curve in this figure corresponds to the

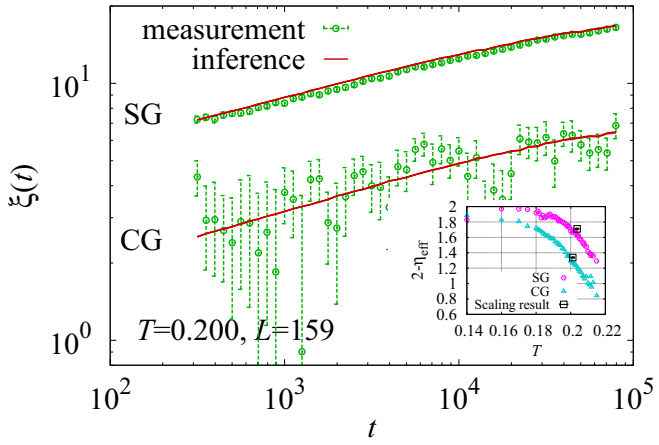

FIG. 3. The correlation length data estimated by the inference and that by the measurements (the second-moment method). Error bars for the inference data are smaller than linewidths. Inset: Temperature dependencies of the effective exponent $\eta_{\rm eff}$. The critical exponent η obtained by the scaling analysis is also plotted.

correlation length. Here, we found the crossover distance, $r_{\rm c}$, dividing the short-range correlation region and the long-range correlation region. Short-range correlations do not depend on t, T, and L. Meaningful information is not included in this region. The growth of the correlation length is only reflected in the long-range correlations. The SG crossover distance ($r_{\rm c} \simeq 9$) is roughly three times greater than the CG one ($r_{\rm c} \simeq 3$). The effects of the periodic boundary conditions appear as the distance approaches $L/2$. We use only the data in the distance range of $2r_{\rm c} < r < L/3$ to exclude influences of short-range correlations and the boundary effects.

The correlation lengths are related to the correlation functions via the following scaling ansatz:

$$f(r,t)/[\xi(t)]^{-1-\eta_{\rm eff}} = \mathcal{F}[r/\xi(t)], \tag{2}$$

where $\mathcal{F}$ denotes the scaling function and $\eta_{\rm eff}$ is the effective scaling exponent. We estimate $\xi(t)$ and $\eta_{\rm eff}$ so that all the $f(r,t)$ data fall onto a single scaling function $\mathcal{F}$. In a Gaussian kernel regression procedure, we set $x_i = r/\xi(t)$, $y_i = f(r,t)/[\xi(t)]^{-1-\eta_{\rm eff}}$, and $\epsilon_i = (\delta y_i)^2$, with i denoting an index number for all the combinations of (r,t). Dozens of $\xi(t)$ data sets are obtained simultaneously from thousands of $f(r,t)$ data sets.

An inset of Fig. 2 shows the result of scaling. We rescaled $\xi(t)$ so that the slope of this plot becomes unity as $\mathcal{F}[r/\xi(t)] \sim \exp[-r/\xi(t)]$. This rescaling defines the unit of the length scale. Figure 3 shows the obtained $\xi(t)$. We compared our inference results with those obtained in the measurement scheme (the second-moment method). The SG data obtained with both methods show a close consistency. On the other hand, numerical instabilities are observed in the CG estimations by the measurement method. In contrast, the inference method solves this instability problem. The effective exponent, $\eta_{\rm eff}$, depends on the temperature reflecting a correction to scaling. We plot the $\eta_{\rm eff}$ values in an inset of this figure. It coincides with the critical exponent at the transition temperature, which will be obtained by the scaling analysis.

TABLE I. Comparisons of our results with previous estimates. Reference [36] is a result of equilibrium simulations, whereas Refs. [10,19] are those of nonequilibrium simulations. References [44,45] are experimental results of AgMn.

	$T_{\rm SG}$	$T_{\rm CG}$	$\nu_{\rm SG}$	$\nu_{\rm CG}$	$\eta_{\rm SG}$	$\eta_{\rm CG}$
This work	0.203(1)	0.201(1)	1.49(3)	1.53(3)	0.28(1)	0.66(1)
Ref. [19]	0.21(1)	0.22(1)	1.1(2)		0.27	
Ref. [36]	0	0.19(1)		1.3(2)		0.8(2)
Ref. [10]	0.203(1)	0.200(1)	1.79(2)	1.57(3)	0.19(1)	0.83(2)
Ref. [44]			1.40(16)		0.46(10)	
Ref. [45]			1.30(15)		0.4(1)	

We apply the dynamic correlation-length scaling analysis [22] using the obtained $[\xi(t),\chi(t)]$ data sets. Figure 4 shows the scaling plot of the SG and CG transitions. We applied the β-scaling method proposed by Campbell *et al.* [43]. We estimated the scaling parameters by the Bayesian inference introduced by Harada [8]. There are 1187 data sets in this figure, and we chose 800 data sets randomly and estimated the scaling parameters for 100 times. We determined the average and the error bar over them. We also show in the inset the same scaling plot using ξ obtained by the measurement method. While it is impossible to perform scaling analysis on the CG data in the measurement method, our inference method made it possible. Estimated transition temperatures and critical exponents are summarized in Table I. The critical temperatures are consistent with previous results. Our values of $\nu_{\rm SG}$ and $\eta_{\rm SG}$ are also consistent with those of the canonical SG materials [44–46]. This evidence suggests that the Heisenberg spin-glass model explains the experiments. On the other hand, results of critical exponents differ from previous simulational results. Reference [10] performed the same scaling analysis as the present work, but obtained physical quantities by a window measurement. The total sample number was almost a half the present work (520 samples at 26 sets of temperatures). The values of critical exponents are very sensitive to the quality of data.

Discussion and summary. The evaluations of physical quantities in numerical studies are generalized to an inference scheme. This is a change of style in numerical investigations on statistical physics. We obtain the most-probable expression for a physical quantity from the discrete raw data. Then, we differentiate or integrate it analytically or numerically to obtain various quantities. We can improve accuracies of physical quantities because they are the product of consistency among many raw data sets. This method has potential applications not only to numerical studies on theoretical models but also to analyses on experimental data. A control of uncertainty in inferred data [5] and validations or extensions of a use of the Gaussian kernel are left for future studies. Gaussian kernel function was chosen in this Rapid Communication based on an assumption that the errors of observed quantities may follow the Gaussian process. This assumption is not always valid and another kernel function needs to be considered in some cases.

In our study on a Heisenberg SG model, we observed a simultaneous SG and CG transition with a common value of exponent ν. Here, one may ask why the SG and CG transitions

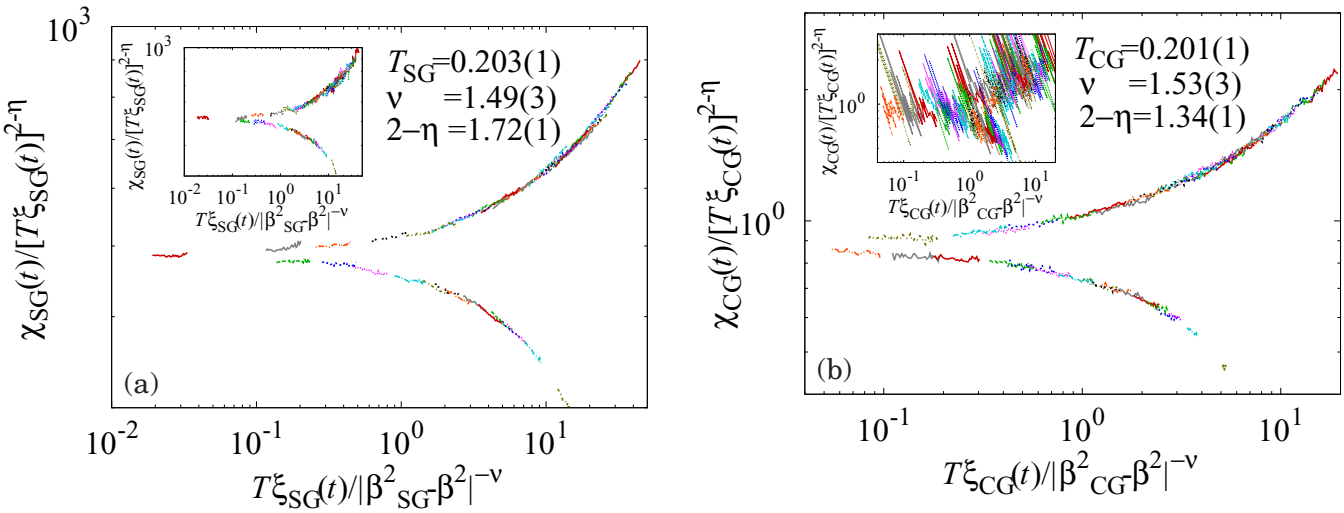

FIG. 4. A scaling plot of (a) the SG transition and (b) the CG transition. Data of 42 sets of temperature ranging from 0.170 to 0.220 are depicted with different color lines. Insets depict the same scaling plot using the correlation length data obtained by the measurements.

have been observed sometimes differently and sometimes simultaneously. In what follows, we clarify this point. There are two important length scales when we discuss the finite-size effect. One is the correlation length and the other one is the crossover length. In the ferromagnetic Heisenberg model, the crossover length is only two to three lattice spacings. Thus, finite-size scaling analysis is possible using data with the minimum size $L = 6$ [47] or 8 [48]. As shown in Fig. 2, the SG crossover length is nine to ten lattice spacings in the Heisenberg spin-glass model. This value is comparable with the correlation length in the present simulation. The necessary length scale should be doubled or tripled under the periodic boundary conditions. This corresponds to a minimum lattice size $L = 20$–30. However, these sizes have been mostly the maximum sizes in the equilibrium simulations. On the other hand, the CG crossover length ($r_c = 2$–3) is almost same as that in the ferromagnetic model. The necessary size may be $L = 6$–8, which has been considered in the equilibrium simulations. This crossover-length issue is the reason why the SG transition was not detected in early simulations, while the CG transition was easily detected.

Acknowledgments. The author would like to thank Chisa Hotta, Naomichi Hatano, and Katsuyuki Fukutani for fruitful discussions. This work is supported by a Grant-in-Aid for Scientific Research from the Ministry of Education, Culture, Sports, Science and Technology, Japan (Grant No. 24540413).

[1] D. P. Landau and K. Binder, *A Guide to Monte Carlo Simulations in Statistical Physics*, 2nd ed. (Cambridge University Press, Cambridge, 2005).
[2] F. Cooper, B. Freedman, and D. Preston, Nucl. Phys. B **210**, 210 (1982).
[3] F. Belletti, M. Cotallo, A. Cruz, L. A. Fernández, A. Gordillo-Guerrero, M. Guidetti, A. Maiorano, F. Mantovani, E. Marinari, V. Martin-Mayor, A. M. Sudupe, D. Navarro, G. Parisi, S. Perez-Gaviro, J. J. Ruiz-Lorenzo, S. F. Schifano, D. Sciretti, A. Tarancón, R. Tripiccione, J. L. Velasco, and D. Yllanes, Phys. Rev. Lett. **101**, 157201 (2008).
[4] H. Suwa and S. Todo, Phys. Rev. Lett. **115**, 080601 (2015).
[5] P. Hennig, M. A. Osborne, and M. Girolami, Proc. R. Soc. London, Ser. A **471**, 20150142 (2015).
[6] G. D'Agostini, Rep. Prog. Phys. **66**, 1383 (2003).
[7] U. Toussaint, Rev. Mod. Phys. **83**, 943 (2011).
[8] K. Harada, Phys. Rev. E **84**, 056704 (2011).
[9] K. Hukushima and I. A. Campbell, arXiv:0903.5026v1.
[10] T. Nakamura and T. Shirakura, J. Phys. Soc. Jpn. **84**, 013701 (2015).
[11] T. Nakamura, J. Phys. Soc. Jpn. **72**, 789 (2003).
[12] T. Nakamura, Phys. Rev. B **71**, 144401 (2005).
[13] C. M. Bishop, *Pattern Recognition and Machine Learning* (Springer, New York, 2006).
[14] William H. Press, Brian P. Flannery, Saul A. Teukolsky, and William T. Vetterling, *Numerical Recipes in C* (Cambridge University Press, Cambridge, 1988).
[15] D. Stauffer, Physica A **186**, 197 (1992).
[16] N. Ito, Physica A **192**, 604 (1993).
[17] Y. Ozeki and N. Ito, J. Phys. A **40**, R149 (2007).
[18] Y. Ozeki and N. Ito, Phys. Rev. B **64**, 024416 (2001).
[19] T. Nakamura and S. Endoh, J. Phys. Soc. Jpn. **71**, 2113 (2002).
[20] T. Yamamoto, T. Sugashima, and T. Nakamura, Phys. Rev. B **70**, 184417 (2004).
[21] T. Nakamura, S. Endoh, and T. Yamamoto, J. Phys. A **36**, 10895 (2003).
[22] T. Nakamura, Phys. Rev. B **82**, 014427 (2010).
[23] *Spin Glasses and Random Fields*, edited by A. P. Young (World Scientific, Singapore, 1997).
[24] N. Kawashima and H. Rieger, in *Frustrated Spin Systems*, edited by H. T. Diep (World Scientific, Singapore, 2004).
[25] J. A. Olive, A. P. Young, and D. Sherrington, Phys. Rev. B **34**, 6341 (1986).
[26] H. Kawamura, Phys. Rev. Lett. **68**, 3785 (1992).

[27] H. Kawamura, J. Phys. Soc. Jpn. **79**, 011007 (2010).
[28] K. Hukushima and H. Kawamura, Phys. Rev. E **61**, R1008 (2000).
[29] F. Matsubara, S. Endoh, and T. Shirakura, J. Phys. Soc. Jpn. **69**, 1927 (2000).
[30] S. Endoh, F. Matsubara, and T. Shirakura, J. Phys. Soc. Jpn. **70**, 1543 (2001).
[31] F. Matsubara, T. Shirakura, and S. Endoh, Phys. Rev. B **64**, 092412 (2001).
[32] M. Matsumoto, K. Hukushima, and H. Takayama, Phys. Rev. B **66**, 104404 (2002).
[33] L. W. Lee and A. P. Young, Phys. Rev. Lett. **90**, 227203 (2003).
[34] L. Berthier and A. P. Young, Phys. Rev. B **69**, 184423 (2004).
[35] M. Picco and F. Ritort, Phys. Rev. B **71**, 100406(R) (2005).
[36] K. Hukushima and H. Kawamura, Phys. Rev. B **72**, 144416 (2005).
[37] I. Campos, M. Cotallo-Aban, V. Martin-Mayor, S. Perez-Gaviro, and A. Tarancón, Phys. Rev. Lett. **97**, 217204 (2006).
[38] L. W. Lee and A. P. Young, Phys. Rev. B **76**, 024405 (2007).
[39] L. A. Fernandez, V. Martin-Mayor, S. Perez-Gaviro, A. Tarancon, and A. P. Young, Phys. Rev. B **80**, 024422 (2009).
[40] D. X. Viet and H. Kawamura, Phys. Rev. Lett. **102**, 027202 (2009).
[41] D. X. Viet and H. Kawamura, Phys. Rev. B **80**, 064418 (2009).
[42] T. Shirakura and F. Matsubara, J. Phys. Soc. Jpn. **79**, 075001 (2010).
[43] I. A. Campbell, K. Hukushima, and H. Takayama, Phys. Rev. Lett. **97**, 117202 (2006).
[44] H. Bouchiat, J. Phys. (Paris) **47**, 71 (1986).
[45] L. P. Lévy, Phys. Rev. B **38**, 4963 (1988).
[46] I. A. Campbell and D. C. M. C. Petit, J. Phys. Soc. Jpn. **79**, 011006 (2010).
[47] P. Peczak, A. M. Ferrenberg, and D. P. Landau, Phys. Rev. B **43**, 6087 (1991).
[48] R. G. Brown and M. Ciftan, Phys. Rev. Lett. **76**, 1352 (1996).